Curve Crossing and Branching Ratios in the Dissociative Recombination of HD^+

D. Zajfman and Z. Amitay
Department of Particle Physics, Weizmann Institute of Science, Rehovot, 76100, Israel

M. Lange, U. Hechtfischer, L. Knoll, D. Schwalm, R. Wester, and A. Wolf
Max-Planck-Institut für Kernphysik and Physikalisches Institut der Universität Heidelberg, D-69029 Heidelberg, Germany

X. Urbain
Département de Physique, Université Catholique de Louvain, Chemin du Cyclotron 2, B1348, Louvain-la-Neuve, Belgium
(Received 27 May 1997)

We present an experimental and theoretical study of the branching ratios in the dissociative recombination of HD^+ with low energy electrons. The results give direct insight into the dynamics of the avoided curve crossing process between the dissociative state and the Rydberg series of the neutral molecule. Excellent agreement between the experimental results and the theory, based on a Landau-Zener formulation of the crossing process, is obtained. [S0031-9007(97)03965-3]

PACS numbers: 34.80.Gs

When a molecular ion collides with a low-energy electron, it can capture the electron and dissociate. The resulting process of dissociative recombination (DR) [1] is one of the most important reactions of molecular ions in astrophysical plasmas. For example, final-state branching ratios and the associated distribution of the fragment kinetic energies after DR are important quantities in planetary ionospheres as they determine fragment escape probabilities from the gravitational field and isotopic concentrations in the atmospheres [2]. The species important in these environments comprise many diatomic and polyatomic molecules, including H_2^+ and its isotopomer HD^+ which are particularly amenable to a detailed theoretical treatment of the recombination reaction.

The DR process $HD^+ + e \rightarrow HD^{**} \rightarrow H + D$ can be viewed as a two-step reaction consisting of the formation, by inverse autoionization, of a doubly excited neutral-molecule state (HD^{**}) and its subsequent dissociation into neutral atomic fragments. Characteristically, a single doubly excited state provides the coupling to the electronic continuum necessary for the capture step, but then the way toward a large number of final states is opened up as, with increasing internuclear distance, the dissociating state crosses the Rydberg series of bound potential energy curves of the neutral molecule which converge to the ionic ground state. In this Letter, we present the first detailed experimental study of this dissociation phase of the DR process, using vibrationally cold ions and a novel three-dimensional, highly resolving fragment imaging method for the final-state analysis. With the data we demonstrate that a surprisingly simple theoretical model, based on Landau-Zener transitions in multiple avoided curve crossings, yields excellent agreement with the observations. Due to its simple structure controlled by few parameters, the theoretical model appears transferable to other molecular systems of more complicated electronic structure; therefore, in connection with the experimental verification, a valuable tool is provided for predicting final-state branching ratios in the DR of molecular ions.

The relevant potential energy curves of $^1\Sigma_g^+$ symmetry for HD [3] are shown in Fig. 1(a) in the quasidiabatic representation [4,5]. The autoionizing state $(2p\sigma_u)^2\ ^1\Sigma_g^+$, populated from the continuum $HD^+(X) + e$, is correlated to the neutral channel labeled $n = 2$, i.e., $H(n = 2) + D(n = 1)$ or $D(n = 2) + H(n = 1)$. On

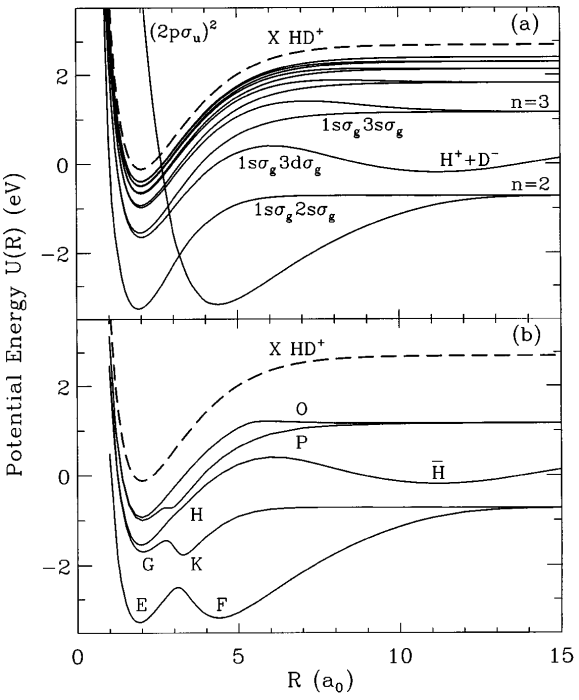

FIG. 1. (a) Relevant quasidiabatic potential curves for HD and HD^+ [3], showing the ground state of HD^+ (dashed line), the Rydberg series for the neutral states, and the $(2p\sigma_u)^2\ ^1\Sigma_g^+$ autoionizing state. (b) Relevant adiabatic potential curves of HD^+ and HD [6].

the other hand, the adiabatic states of symmetry $^1\Sigma_g^+$ [6], shown in Fig. 1(b), must strictly obey the noncrossing rule of von Neumann and Wigner [7]. In the DR process, diabatic transitions occur at the avoided crossings between these adiabatic states so that various final states can be populated if energetically accessible, as was discussed by many authors [1,8]. The size of the *total* DR cross section can be predicted rather well without considering the distribution of flux at the avoided crossings. Cross section calculations were found to be in good agreement with recent measurements using relaxed molecular ions in storage rings [9–12]. No experiments so far have dealt with the partial cross sections into different final states for low-energy DR via the $(2p\sigma_u)^2$ curve, which reflect the diabatic transition rates at the avoided crossings. It is important to point out that these transitions also form an integral part of other types of dissociation processes (such as photodissociation) and as such their understanding is of high relevance in the unfolding of the dynamics of molecular breakups.

In this work we have measured and calculated the branching ratios for DR of HD^+ in the range of center-of-mass (c.m.) electron energies E_e of 0–2.5 eV, combining the heavy-ion storage ring technique with a new three-dimensional imaging method for the molecular fragments. Using storage rings one can produce fast and intense, vibrationally cold molecular ion beams [9–15]. The first experiment probing the branching ratios into different atomic final states in molecular DR was carried out by our group [16] using a two-dimensional fragment imaging technique. Data obtained in this earlier work showed that at $E_e = 0$ DR of HD^+ leads only to the $n = 2$ channels.

The Test Storage Ring (TSR) [17], located at the Max-Planck-Institut für Kernphysik, Heidelberg, was filled by a beam of 2-MeV HD^+ ions from a Van de Graaff accelerator and a standard Penning ion source. The basic experimental setup has been described previously [15] and will be presented here only shortly. Typically 10^7 particles circulated in the ring with a lifetime of $\approx$15 s. The circulating ion beam was merged with the 5-cm diam, quasimonochromatic electron beam of the electron cooler over a length of 1.5 m, providing electrons at a typical density of 2×10^6 cm^{-3} and a temperature of $\approx$0.015 eV in the comoving reference frame. An 80-mm diam chevron microchannel-plate (MCP) detector was mounted straight ahead of the cooler section at a distance of 6 m to detect the neutralized particles from the cooler region. Each impact on the MCP produced a light spot on a phosphor screen located behind the MCP. The positions and times of impact of each of the fragments were analyzed using a new three-dimensional position and time detector [18]. In this detector setup, a CCD camera digitizes the spatial coordinates with a resolution of 50 μm; in addition the screen is imaged onto a 16-strip multianode photomultiplier which measures the time of impact of each fragment with a resolution of 170 ps. From the relative position d_{2D} and the time difference Δt between the impacts for each pair of H and D fragments, their three-dimensional distance d_{3D} upon arrival at the detector can be determined using the relation $d_{3D}^2 = (v_0 \Delta t)^2 + d_{2D}^2$, where v_0 is the ion beam velocity.

The kinetic energy release E_k in the c.m. frame is represented by the difference between the c.m. electron energy E_e and the internal (electronic) energy of the fragments, measured relative to the initial (rovibrational) energy level of HD^+. Recombination events associated with a kinetic energy release E_k yield the three-dimensional fragment distance

$$d_{3D} = L(M/\sqrt{m_1 m_2})\sqrt{E_k/E_0}, \qquad (1)$$

where E_0 is the ion beam energy, L the distance from the dissociation point to the detector, M the molecular ion mass, and m_1 and m_2 are the fragment masses. The distribution of the measured three-dimensional distances d_{3D} for events with a given fixed E_k is broadened in this experiment by the finite extension of the interaction region (1.5 m $\approx$ 23% of the average distance $L_0 =$ 6.47 m) and by the 170-ps time resolution ($\approx$17% of the typical relative time difference of $\approx$1 ns). The measured d_{3D} distributions also contain some background coming mainly from the bending regions of the electron cooler [15], which produce DR events with higher-energy electrons, but these events mostly have higher kinetic energy releases. The measurement of the time difference Δt allows one to suppress completely random coincidences between two unrelated single fragments produced by collisions with the residual gas.

The three-dimensional distance spectra as measured for three different electron energies in a time interval of 1–15 s after the injection are shown in Fig. 2. Background subtraction and correction for the efficiency of the photomultiplier, considering its detailed anode structure [18], have been applied. The expected relative distances d_{3D} for recombination into the different final channels $n = 2, 3, 4$, calculated for HD^+ ions in the rovibrational ground state and for $L = L_0$, are marked with arrows. As can be seen, the different contributions show up as separate peaks centered close to the calculated positions, which confirms both the relaxation of the ions stored in the ring and the resolution obtained in the fragment imaging. At $E_e = 0$ [Fig. 2(a)], only a single peak is found as only the $n = 2$ final channels are accessible. At $E_e = 1.81$ eV [Fig. 2(b)] the $n = 3$ channels are accessible and indeed formed with relatively high branching ratio; at $E_e = 2.12$ eV [Fig. 2(c)], also the $n = 4$ channels are open and do yield a sizeable contribution. Hence, it is immediately apparent that DR leads to substantial production of excited products as soon as the electron energy is above the threshold for their formation.

For the whole series of measurements, the branching ratios were obtained by integrating the surfaces of the observed peaks and normalizing the results to yield a unity sum. The results for $E_e > 1.1$ eV are shown in

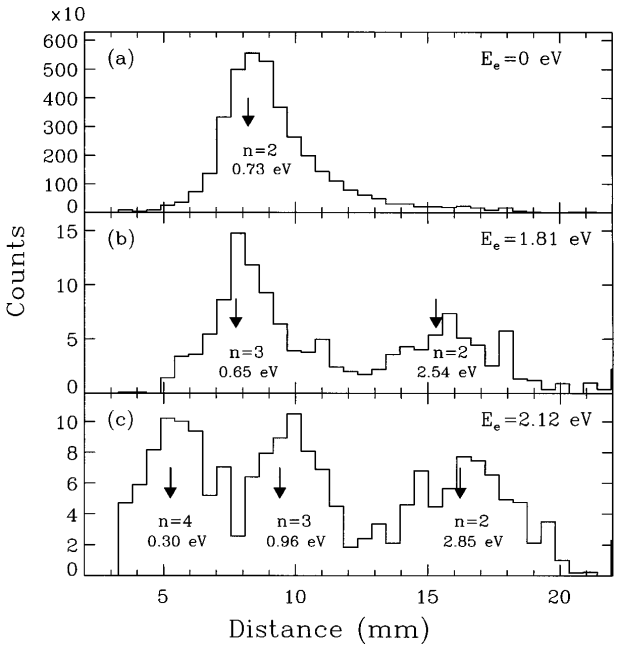

FIG. 2. Distributions of the three-dimensional distance between the DR fragments as measured for different electron energies: (a) $E_e = 0$, (b) $E_e = 1.81$ eV, and (c) $E_e = 2.12$ eV. Each peak in the spectra is marked with its corresponding final state and kinetic energy release E_k, and with an arrow pointing to the expected three-dimensional distance for dissociation from the average distance L_0 (see text).

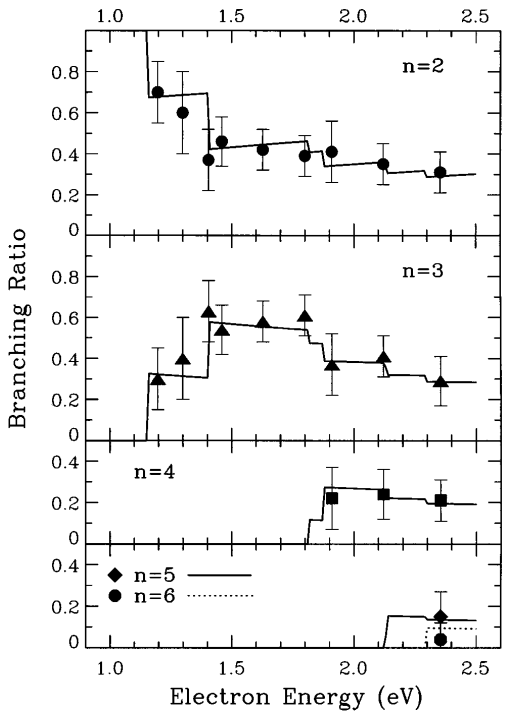

FIG. 3. Branching ratios for the DR of HD^+ as a function of the electron energy for the final states $n = 2$, $n = 3$, $n = 4$, and $n = 5, 6$. The symbols are the experimental results and the lines the results of the calculation. The theory for $n = 5$ and 6 is shown by full and dotted lines, respectively.

Fig. 3; for $E_e \leq 1.1$ eV only the neutral channel with $n = 2$ is populated. The error bars are mainly due to the background subtraction and to the uncertainties in the detector efficiencies for different fragment distances. The results show that the opening of each new channel occurs very fast at its energetic threshold. However, when more and more channels open with increasing electron energy, no single asymptotic state is really predominant.

In order to analyze the results in a more quantitative way, we have developed a theoretical description of the branching process based on the Landau-Zener formulation. As described above, the $(2p\sigma_u)^2\ ^1\Sigma_g^+$ state (the first member of the Q_1 series of diexcited states converging to the $2p\sigma_u$ ionic core) has been recognized for long as the main route toward dissociative recombination at low energy for H_2^+ and its isotopomers [19,20]. The diabatic curve of this state can be easily traced in the bound part of the spectrum since it produces a characteristic pattern of double minima [see Fig. 1(b)]. Precisely, this avoided crossing series has been used to diabatize the set of potential energy curves to obtain that of the $(2p\sigma_u)^2\ ^1\Sigma_g^+$ resonant state and, as a by-product, its autoionization width Γ through the relation $\Gamma = 2\pi \sum_{l=s,d} |V_l|^2$, where V_l stands for the electronic interaction with the scattering continua s and d. The latter parameters are related to the two-state interaction V_{nl} responsible for the avoided crossing between the $(2p\sigma_u)^2$ state and a given Rydberg state through the Rydberg formula $V_l = (n - \mu_l)^{3/2} V_{nl}$, where μ_l is the quantum defect associated with the $1s\sigma_g\, nl\sigma_g$ series. The parameters Γ, V_l, and V_{nl} are functions of the internuclear distance R. Hazi *et al.* [21] made use of these relations to extract the width of the $(2p\sigma_u)^2$ resonance and thereby confirm their *ab initio* calculations. A multichannel quantum-defect analysis of the *ab initio* potential energy curves has been performed by Ross and Jungen [22], yielding parameters in good agreement with the previous determination.

Provided $(2p\sigma_u)^2$ is the only diexcited state to be populated by the low energy DR considered here ($E_e < 2.5$ eV), the branching ratio problem is restricted to the multiple curve crossing scheme depicted in Fig. 1(a), where the lowest Q_1 state crosses the two Rydberg series $1s\sigma_g\, ns\sigma_g$ and $1s\sigma_g\, nd\sigma_g$ in a very narrow range of internuclear distance ($2.6a_o < R < 3a_o$). At such short distances, the configuration states, i.e., singly and doubly excited configurations of molecular orbitals, constitute a diabatic basis. It seems therefore appropriate to adopt a Landau-Zener formulation for the transition probabilities associated with the successive crossing points. The relevant parameters were already given in the early work of Hazi *et al.* [21], and are used here to treat the redistribution of flux taking place along the Rydberg series, following the multistate-curve-crossing model (MSCC) of Cohen [23].

For the final results the assignment of correct asymptotic final states to the different configuration states within the two $^1\Sigma_g^+$ Rydberg series is of particular importance. The case of the s series is relatively simple, each state

dissociating into H + D(n) or D + H(n) according to the principal quantum number of its Rydberg orbital $ns\sigma_g$. The fact that both the $(2p\sigma_u)^2$ and the $1s\sigma_g\,2s\sigma_g$ configurations dissociate into identical atomic states brings in some interference, as discussed by Urbain *et al.* [3]. The d series is characterized by the phenomenon of orbital promotion, by which the $nd\sigma_g$ orbital is correlated to a lower separated atom limit, H + D($n-1$) or D + H($n-1$), due to the (quasi) degeneracy existing between these two arrangements. This effect produces the humps exhibited by the states $H, \bar{H}\ ^1\Sigma_g^+$, and $O\ ^1\Sigma_g^+$ [see Fig. 1(b)]. According to the diabatic correlation diagram, the $1s\sigma_g\,3d\sigma_g$ configuration state should dissociate into H + D($n=2$) or D + H($n=2$). However, its avoided crossing with the ionic state at $R = 11a_o$ makes it turn around and exchange its correlation with that of the $(2p\sigma_u)^2$ state. The first member of the d series therefore has not been considered as a neutral dissociation channel.

In the present description, the combination of transition probabilities is restricted to all the open channels at a given total energy, that is, above their dissociation limit *or* above the humps existing in the d potential curves. Since the $1s\sigma_g\,3d\sigma_g$ state leads to ion pairs above 1.9 eV and is hindering the dissociation into neutrals below that limit, it is taken into account as an ionic open channel for all energies by artificially lowering its dissociation limit. Its main effect is to lower the branching toward the $n = 2$ channels, as it lies below all the curves feeding the higher dissociation limits.

The results of this Landau-Zener calculation are shown in Fig. 3 together with the measured branching ratios. The calculated curves clearly reveal the redistribution of flux at the thresholds for the different final states. Moreover, the flux going via the $1s\sigma_g\,4d\sigma_g$ and $1s\sigma_g\,5d\sigma_g$ states into the final channels $n = 3, 4$ shows up at additional thresholds related to the humps in the respective potential curves. The agreement of this theoretical model with the experimental data is excellent for all channels over the whole energy range covered by the experiment. In particular, the experiment confirms the additional rise of the $n = 3$ branching ratio at the threshold for the path via $1s\sigma_g\,4d\sigma_g$. The good agreement also confirms the values of the interaction matrix elements V_{nl} between the doubly excited dissociative state and the molecular Rydberg states, which entered the curve-crossing model, and, to less extent, verifies the correctness of the relevant HD^+ quasidiabatic potential curves. As described above, these V_{nl} couplings are directly related to the important value of the $(2p\sigma_u)^2$ autoionization width. In that context, it is also important to mention that they are important ingredients in the so-called indirect DR [24,25], and in vibrational transitions of HD^+ [26].

The Landau-Zener calculation for HD^+ and its possible extension to other systems provides a useful method for predicting the distribution of fragment energies and the internal excitation states of the fragments after DR and other similar breakup processes. Radiative emission, fragment reactivities, and fragment escape probabilities from gravitational potentials can be modeled with this information. For the specific case of HD^+, both experiment and theory show that a considerable part of the fragments acquire a high degree of internal excitation and correspondingly low kinetic energies as soon as the related channels are energetically open. Similar studies on other systems appear desirable in order to verify if this behavior generally occurs in molecular dissociation.

This work has been funded in part by the German Federal Minister for Education, Science, Research and Technology (BMBF) under Contract No. 06 HD 854 I, the EU/HCM program, and by the German Israel Foundation (GIF) under Contract No. I-0452-200.07/95. X. U. is Research Associate of the Belgian National Fund for Scientific Research (FNRS).

[1] J. N. Bardsley and M. A. Biondi, Adv. Mol. Phys. **6**, 1 (1970).
[2] J. L. Fox, in *Dissociative Recombination: Theory, Experiment and Applications*, edited by B. R. Rowe, J. B. A. Mitchell, and A. Canosa (Plenum Press, New York and London, 1993), p. 219.
[3] X. Urbain, A. Cornet, F. Brouillard, and A. Giusti-Suzor, Phys. Rev. Lett. **66**, 1685 (1991).
[4] V. Sidis and H. Lefebvre-Brion, J. Phys. B: At. Mol. Phys. **4**, 1040 (1971).
[5] A. Giusti, J. Phys. B: At. Mol. Phys. **13**, 3867 (1980).
[6] L. Wolniewicz and K. Dressler, J. Chem. Phys. **100**, 444 (1994).
[7] J. von Neumann and E. P. Wigner, Physik. Z. **30**, 467 (1929).
[8] J. B. A. Mitchell, Phys. Rep. **186**, 215 (1990).
[9] P. Forck *et al.*, Phys. Rev. Lett. **70**, 426 (1993).
[10] T. Tanabe *et al.*, Phys. Rev. Lett. **75**, 1066 (1995).
[11] C. Strömholm *et al.*, Phys. Rev. A **52**, R4320 (1995).
[12] L. H. Andersen *et al.*, Phys. Rev. A **55**, 2799 (1997).
[13] P. Forck *et al.*, Phys. Rev. Lett. **72**, 2002 (1994).
[14] Z. Amitay *et al.*, Phys. Rev. A **53**, R644 (1996).
[15] Z. Amitay *et al.*, Phys. Rev. A **54**, 4032 (1996).
[16] D. Zajfman *et al.*, Phys. Rev. Lett. **75**, 814 (1995).
[17] D. Habs *et al.*, Nucl. Instrum. Methods **B43**, 390 (1989).
[18] Z. Amitay and D. Zajfman, Rev. Sci. Instrum. **68**, 1387 (1997).
[19] G. V. Dubrovsky and V. D. Ob'edkov, Sov. Astron.-AJ **11**, 305 (1967).
[20] C. Bottcher, J. Phys. B: At. Mol. Phys. **9**, 2899 (1976).
[21] A. U. Hazi, C. Derkits, and J. N. Bardsley, Phys. Rev. A **27**, 1751 (1983).
[22] S. C. Ross and Ch. Jungen, Phys. Rev. A **49**, 4353 (1994).
[23] J . S. Cohen, Phys. Rev. A **13**, 99 (1976).
[24] A. P. Hickman, J. Phys. B: At. Mol. Phys. **20**, 2091 (1987).
[25] I. F. Schneider, O. Dulieu, and A. Giusti-Suzor, J. Phys. B: At. Mol. Phys. **24**, L289 (1991).
[26] K. Nakashima, H. Takagi, and H. Nakamura, J. Chem. Phys. **86**, 726 (1987).